Lattice simulations of quark forces at finite temperature

Leo I. Unger*
Department of Physics, Columbia University, New York, New York 10027
(Received 15 October 1992)

We have performed a systematic study of the static quark-antiquark potential in the presence of light dynamical fermions. The potential has been extracted from measurements of Wilson line correlation functions on a $16^3 \times 4$ lattice. In the low-temperature QCD phase the effects of dynamical fermions on the confining quark potential are demonstrated. In the high-temperature plasma phase we analyze the screening mass for different quark masses and different numbers of flavors at a range of temperatures. It is found that the inclusion of dynamical fermions enhances screening effects significantly. The screening mass shows a strong temperature dependence and our results suggest that J/ψ suppression might be effective for temperatures $T \simeq T_c$.

PACS number(s): 12.38.Gc, 12.38.Mh, 12.40.Qq, 14.40.Gx

I. INTRODUCTION

A quantitative theoretical understanding of the heavy quark potential based on QCD is of fundamental interest for several reasons.

(1) Heavy quark systems such as those consisting of charm or bottom quarks can be meaningfully described as a nonrelativistic problem. Experimental spectroscopy data of bound heavy quark systems such as charmonium (J/ψ) and bottomonium (Υ) can be compared with the bound states computed from a potential via the Schrödinger equation. This also allows a prediction of the anticipated toponium spectrum.

(2) The quantitative analysis of quark forces yields important information about the mechanism of confinement. According to our current understanding, the confinement of color charges is a consequence of the non-Abelian character of the gauge interaction in QCD. The structure of the QCD vacuum at low temperature is such that the chromoelectric field lines between quarks are concentrated within narrow flux tubes. As long as vacuum polarization effects do not screen the color charges the potential of a quark-antiquark ($q\bar{q}$) pair will increase with distance between the two sources. At high temperature, however, the system is in a deconfined phase and the $q\bar{q}$ interaction takes the form of a Yukawa potential characterized by a screening mass.

(3) According to one of the predictions of QCD a quark-gluon plasma is formed when the vacuum is heated to a temperature of a few hundred MeV. This state is characterized by asymptotic freedom, deconfinement, and chiral symmetry restoration. Efforts to create this new form of matter in relativistic heavy ion collision experiments are currently under way. An experimental signature for plasma formation might be the suppression of J/ψ particle production above the transition temperature [1]. The formation of a J/ψ in the plasma depends on the color screening length of the medium. To determine the screening length as a function of temperature requires a detailed analysis of the long-distance behavior of the potential.

In the temperature regime of interest perturbative QCD is not applicable because of infrared problems. Nonperturbative studies of QCD at finite temperature can be performed by introducing a lattice regularization of the theory.

In the following we will discuss Monte Carlo results for the static $q\bar{q}$ system based on the Wilson line correlation method. We have measured Wilson line correlations for both the low-temperature confining phase and the high-temperature deconfined phase, with the main focus on the deconfined plasma phase. In our study we only include the spin-independent part of the potential.

In Sec. II we describe the computational method, Secs. III and IV contain our results for the confined and plasma phase, respectively, in Sec. V we analyze the main results for the potential in the plasma phase, and in Sec. VI some brief conclusions are given.

II. COMPUTATIONAL METHOD

Our simulations were performed on a $N_s^3 \times N_t$ Euclidean lattice with $N_s = 16$ and $N_t = 4$. The gauge field configurations are generated according to the N_f-flavor lattice QCD action

$$S = -\frac{\beta}{3} \sum_{\mathcal{P}} \mathrm{Re\,tr}\, U_{\mathcal{P}} - \frac{N_f}{4} \ln \det(D + m), \qquad (1)$$

where $U_{\mathcal{P}}$ is the product of the link matrices forming the boundary of the elementary plaquette $\mathcal{P}$. The Kogut-Susskind Dirac operator is given by

$$(D\phi)_n = \frac{1}{2} \sum_{\mu} \eta_{n,\mu} (U^{\dagger}_{n,\mu} \phi_{n+\mu} - U_{n-\mu,\mu} \phi_{n-\mu}),$$

*Current address: Thinking Machines Corp., 245 First Street, Cambridge, MA 02142.

where $U_{n,\mu}$ and $\eta_{n,\mu}$ are the link matrices and Kogut-Susskind sign factors associated with the link at site n with direction μ.

There are two commonly used methods to measure the heavy quark potential on the lattice: Wilson loops and Wilson line correlations. In the first method the potential between a $q\bar{q}$ pair is extracted, up to an additive constant, from the expectation value of a planar Wilson loop $W(r,T) = \prod_{l \in C} U_l$ whose contour C is a rectangle, extending in the space direction a distance r and in the time direction a distance T:

$$V(r) = -\lim_{T\to\infty} \frac{1}{T} \ln W(r,T) \,. \tag{2}$$

Since in Eq. (2) the Euclidean time extent stretches out to infinity one obtains the potential at zero temperature [2].

In the second method one measures the correlation function

$$\Gamma(\mathbf{r}) = \left\langle \frac{1}{N_s^3} \sum_{\mathbf{n}} P(\mathbf{n}) P^*(\mathbf{n}+\mathbf{r}) \right\rangle \tag{3}$$

of two Wilson lines P to determine the free energy $F_{q\bar{q}}(\mathbf{r})$ of a $q\bar{q}$ pair separated by a spatial distance $\mathbf{r}$:

$$\Gamma(\mathbf{r}) \propto e^{-F_{q\bar{q}}(\mathbf{r})/T} . \tag{4}$$

The Wilson line correlation method has two advantages over the use of Wilson loops: First, the potential can be obtained at any temperature, and second, the procedure of fitting and extracting the potential is more straightforward since in practice it is usually difficult to subtract the self-energy contributions in Eq. (2). The disadvantage of this method is that the signal-to-noise ratio becomes very small for large N_t since $\langle P \rangle \sim \exp(-N_t F_q)$. For the pure gauge theory there exists a "multihit" method which reduces the noise significantly [3], so that measurements for $N_t = 24$ and beyond are possible. For QCD with dynamical fermions no such variance reduction technique is known and the direct measurement of Wilson line correlations beyond $N_t = 4$ or 6 becomes difficult.

We have measured $\Gamma(\mathbf{r})$ for all $\mathbf{r} = (n_x, n_y, n_z)$, with $0 \le n_x, n_y, n_z \le 8$, which gives us a set of 729 points (because of the periodicity of the lattice the remaining $\mathbf{r}$'s are equivalent). Although the inclusion of all different $\mathbf{r}$'s makes the computation quite demanding for a spatial volume of 16^3 points, the complete information about the correlation function allows for detailed analysis and better statistics. It is possible to investigate the rotational symmetry of the system and by considering diagonal points one can enlarge the fitting range of $r = |\mathbf{r}|$ by a factor of $\sqrt{3}$. Since the link variables are gauge transformed into temporal gauge after each time step by the updating program, the actual computation involves correlating the traces of the SU(3) matrices in a single time slice. Correlations are calculated between every pair of space points in the lattice and then averaged over pairs that are separated by a vector $\mathbf{r}$. Measurements have been performed on the gauge configurations obtained after each trajectory of $\frac{1}{2}$ unit of time.

The reported results are part of a series of finite temperature simulations undertaken by the lattice QCD group at Columbia. These studies were performed with different numbers of quark flavors and the quark mass region was explored down to a value of $m = 0.01$. Details of the numerical algorithms can be found in [4,5]. The calculations were carried out on the 256-node Columbia parallel supercomputer, a two-dimensional array of processors with fast nearest-neighbor communication [6]. The dynamical fermion algorithm runs at a sustained speed of 6.4 Gflops. For four flavors with equal mass a first-order phase transition was demonstrated for mass values of m=0.01, 0.025, 0.0375, and 0.05 [5]. The calculation with three flavors of mass $m = 0.025$ shows also a first-order transition [4].

III. HEAVY QUARK POTENTIAL IN THE CONFINED PHASE

In the pure gauge sector of QCD the forces between quarks can be well described in terms of a string model. In the confined phase the $q\bar{q}$ potential is expected to rise linearly with the separation of the quarks:

$$V(r) = V_0 + \sigma r \,. \tag{5}$$

The proportionality constant σ is usually referred to as the string tension. To describe the short-distance behavior a Coulomb potential term $\frac{\alpha}{r}$ can be added to Eq. (5). As one of the main analytic results of lattice gauge theory it can be proved that, for pure gauge theory, quarks are confined in the strong coupling limit and the string tension associated with the confining potential can be calculated. There have also been a large number of Monte Carlo simulations for pure QCD to extract a value for the string tension numerically (see, e.g., [7]).

For full QCD the situation is significantly different. With the inclusion of dynamical fermions vacuum polarization effects become important. When the distance between static quarks becomes sufficiently large, the creation of $q\bar{q}$ pairs is possible.

For the confined QCD phase we have Wilson line correlation data for two and four flavors. In both cases the value of the quark mass is $m = 0.01$. For four flavors a first-order phase transition occurs at $\beta = 4.95$ [5]. At this coupling we have runs, starting from ordered and disordered configurations which remain in distinct phases during the whole evolution. Correlation measurements of the disordered start run provide information about the system in the confined phase. For two flavors no transition has been observed [4], but a continuous crossover between the two phases occurs around $\beta = 5.265$.

In Fig. 1 we show the static $q\bar{q}$ potential for two flavors at $\beta = 5.25$. The data represent the last 400 units of time of a run with 500 time units. The first 100 have been discarded for equilibration. We should note that the depicted interquark potential does not represent the effects of image charges that occur as a result of the periodic boundaries of the lattice. As such the potential is

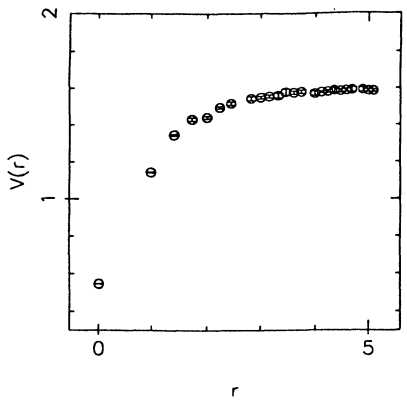

FIG. 1. Static $q\bar{q}$ potential for $N_f = 2$, $m = 0.01$, $\beta = 5.25$. The asymptotic value predicted by the cluster theorem is 1.59.

represented in a range r, where $r < N_s/2$.

Figure 2 shows the potential in the confined phase for four flavors at $\beta = 4.95$. It represents measurements from 250 units of time.

We can clearly see that $V(r)$ rises near the origin and then flattens out after ~ 3 lattice spacings to reach an asymptotic value. This value is predicted by the cluster theorem which implies that $V(r) = -T\ln(|\langle P\rangle|^2)$ for large r. Our measurements of this value give 1.59 for $N_f = 2$ and 1.53 for $N_f = 4$.

The graphs show convincingly the effects of the dynamical fermions on the $q\bar{q}$ potential. In the quenched approximation ($m = \infty$) the potential plotted as a function of r gives a linearly rising curve (except near the origin where the linear potential is modified by a Coulomb term) [8].

We can demonstrate the contrast between the full QCD potential and the quenched potential by trying to fit our data to the functional form used in the case of the pure gauge theory:

$$\langle P(0)P^*(r)\rangle = \sum Ze^{-\sigma r/T - \ln(r)}. \tag{6}$$

The sum includes the eight effective color charges. The $\ln(r)$ term takes into account excitations at finite temperature.

From the plotted fitting data in Fig. 3 we can see that the correlation function abruptly changes its behavior near r=4–5. Within a few lattice spacings from the origin there is a decrease but for $r \geq$4–5 the correlation data has an almost constant nonzero value. This is in sharp contrast to the pure gauge theory case where the correlation function in an exponential falloff smoothly approaches zero [8,9].

By comparing Figs. 1 and 2 we can recognize a certain difference in the form of the potentials for two and four flavors. The two-flavor potential flattens out more slowly than the four-flavor potential. It reaches an approximately constant value near $r \simeq 3.5$, whereas in the four-flavor case the plateau has already been reached near $r \simeq 3.0$. This shows the effect of increased screening of the color charges when changing the number of flavors from 2 to 4.

We can distinguish two different regions: The region $r > 4$ gives the potential between two colorless $q\bar{q}$ pairs. The interaction between these two mesons can be described by some effective exchange of light mesons, such as π and ρ. In principle it should be possible to calculate the masses of the exchanged particles from the data of the potential at large distances and to compare it with results of phenomenological models. From the graphs it would appear that the string breaks if the quarks are pulled further apart than ~ 3 lattice units. In the region $r < 3$ one might describe the physics of the static $q\bar{q}$ system by some effective string picture. Although the definition of the string tension assumes an asymptotically large separation of the quarks we can fit the functional form

$$V(r) = -\frac{\alpha}{r} + \sigma r + T\ln r \tag{7}$$

to the data points near the origin to obtain an effective string tension. Here we have modified (6) by adding a Coulomb term to account for the short-distance behavior of the potential.

For two flavors of mass 0.01 at $\beta = 5.25$ we obtain

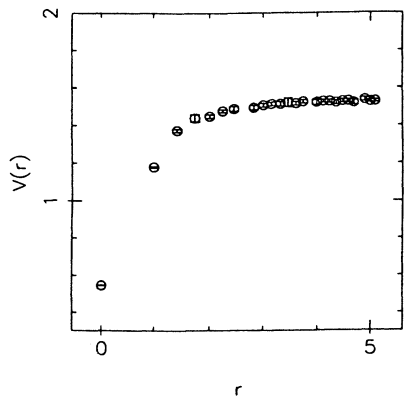

FIG. 2. Static $q\bar{q}$ potential for $N_f = 4$, $m = 0.01$, $\beta = 4.95$. The asymptotic value predicted by the cluster theorem is 1.53.

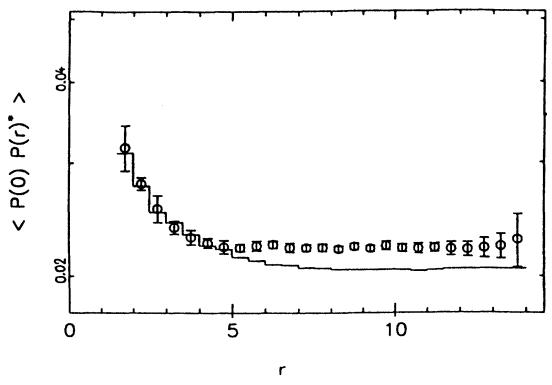

FIG. 3. String tension fit for $N_f = 4$, $m = 0.01$, $\beta = 4.95$. The lower fitting range is $r_{\min} = 2.0$. The data shown are binned into intervals of $\Delta r = 0.5$.

$\alpha = 6.70 \pm 0.87, \sigma = 0.14 \pm 0.10$ for a fitting range that lies between 1.8 and 4.0.

For pure gauge theory on a $24^3 \times 4$ lattice at $\beta = 5.65$ the string tension is $\sigma = 0.40$ [9]. Both of these values of β are slightly below β_c. We see that the effective string tension computed in full QCD is substantially lower than the string tension of the pure gauge theory, consistent with the idea that polarization by dynamical fermions produces a significant weakening of the string.

Our results for the $q\bar{q}$ potential in the confined phase match well with those obtained by Faber *et al.* [10]. They have determined the confined potential on a $8^3 \times 4$ lattice for three flavors and a series of quark masses from $m = \infty$ down to $m = 0.1$. Their value of β is 5.2 (the transition is at $\beta_c = 5.3$). They observe increasing screening effects as the quark mass is decreased. Our measurements for $m = 0.01$ agree within errors with their $m = 0.1$ results and extend them, showing that $V(r)$ approaches a constant for $r \geq 4.0$.

IV. COLOR SCREENING IN THE PLASMA PHASE

In this section we concentrate on the physics of the high-temperature chirally symmetric phase of QCD. In this phase, quarks and gluons are deconfined and may form a weakly interacting gas. It is believed that this state of matter existed at an early stage of the universe. Experimental efforts to create a quark-gluon plasma in heavy ion collisions are under way at CERN and Brookhaven.

At the QCD phase transition the heavy quark potential changes from a confining $q\bar{q}$ potential in the hadronic phase to a Debye screened Coulomb potential in the plasma phase. At low temperature the rising confining potential discussed in the last section favors the formation of heavy bound quark systems such as the charmonium (J/ψ) and bottomonium (Υ) families. These resonances may still exist in the deconfined phase as bound states of a screened Coulomb potential until the temperature and/or density become so high that increased screening effects prevent binding.

A crucial question is what observable signatures can provide information about the creation of a quark-gluon plasma. One proposal is trying to relate the screening properties of the dense hadronic system to a suppression of J/ψ production [1]. If nuclear collisions result in a quark-gluon plasma the produced $c\bar{c}$ pairs find themselves in a deconfining environment. The answer to the question whether bound states exist in the plasma phase depends on the size of the Debye color screening radius r_D. If r_D is smaller than the binding radius of the J/ψ then no such states are formed. A semiclassical analysis, using the nonrelativistic Schrödinger equation, yields a critical value of 0.53 GeV for the Debye screening mass $\mu = 1/r_D$ [11]. For larger values of μ no bound $c\bar{c}$ states should exist.

The expected lifetime of the plasma is on the order of 10^{-23} s. If one assumes that the c and $\bar{c}$ quarks thermalize then it will be unlikely for them to recombine as the plasma cools down. They go into open charm channels which leads to the production of mesons with only one charmed quark, such as $c\bar{u}$ and $\bar{c}u$. One might therefore expect J/ψ suppression in the final state of the collision.

In the context of such a description of heavy ion collisions it is therefore clear that an investigation of the temperature dependence of the $q\bar{q}$ potential in the plasma phase, and in particular of the screening mass μ, is of great interest.

At high temperature perturbation theory yields, for the potential,

$$V(r,T) \simeq \frac{1}{r^2} e^{-2\mu r} , \tag{8}$$

where [12,13]

$$\mu = \sqrt{\frac{6+N_f}{6}} g(T) T . \tag{9}$$

However, the nature of the physical system near the transition is highly nonperturbative and it is more appropriate to use a general ansatz of the form

$$\frac{V(r,T)}{T} = \frac{g^2(T)}{(rT)^n} e^{-\mu r} . \tag{10}$$

Previous calculations [9,14,15] have shown that for temperatures not much higher than T_c, $n = 1$ gives the best agreement with the numerical data. Since our calculations focus on temperatures near the transition region we choose in the following to fix $n = 1$ and fit our data to the potential:

$$V(r) = g^2 \frac{e^{-\mu r}}{r} . \tag{11}$$

In order to extract the long-distance behavior of the potential it is important to fit the data for distances as large as possible.

A. Fitting procedure

Before presenting results we describe here our fitting procedure.

Since our $N_s = 16$ lattice is periodic, the minimum distance between the two Wilson lines can only vary between $r = 1.0$ and $r = 8.0\sqrt{3}$. After discarding the nonequilibrium part (usually 100–200 units of time), the raw data is averaged into 729 data points and their corresponding errors. We perform a least-squares fit of all points which fall within the specified range $[r_{\min}, r_{\max}]$. The function to be minimized is

$$S = \sum_{\mathbf{r}} \frac{[c(\mathbf{r}) - f(\mathbf{r})]^2}{[\Delta c(\mathbf{r})]^2} . \tag{12}$$

$c(\mathbf{r})$ is the correlation data, $f(\mathbf{r})$ the fitting function, and $\Delta c(\mathbf{r})$ the error of the data (S does not take into account the fact that the errors at different values of $\mathbf{r}$ are correlated). The fitting function includes the effects of the seven image charges stemming from the periodicity of the lattice.

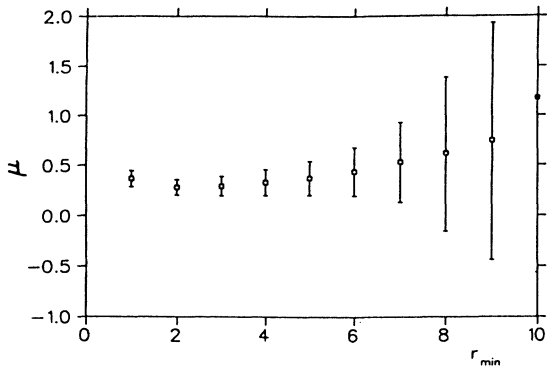

FIG. 4. Dependence of μ on the minimum fitting radius $r_{\min}$. Wilson line correlation data for $N_f = 4$, $m = 0.05$, $\beta = 5.04$ are fitted to the potential $g^2 \exp(-\mu r)/r$.

Errors are calculated with the jackknife method. The correlation data is averaged into N=8–10 blocks and N separate fits are performed by leaving out the first, the second, etc., of the N data blocks. The error on the fitted parameters is calculated from the distribution of those parameters obtained from each of the N fits.

The fitted parameters μ and g^2 depend on the fitting range, i.e., on the minimum and maximum fitting radii $r_{\min}$ and $r_{\max}$. The main dependence is on $r_{\min}$. Since we are interested in the asymptotic behavior of the fitting function we should choose $r_{\min}$ as large as possible. This, however, is impeded since the errors of the correlation data become very large for large distances (see, e.g., Fig. 7), resulting in large errors on the fitted parameters. We hope to find a series of intervals $[r_{\min}, r_{\max}]$ for which the fitting results are stable and have small errors. This is generally the case for $2.0 \lesssim r_{\min} \lesssim 4.0$. By plotting the parameters as a function of $r_{\min}$ (or $r_{\max}$) one attempts to determine the fitting range that yields the best results. An example of this procedure is shown in Fig. 4. As is generally the case, for $r_{\min} = 1.0$ the fitting results are larger than for $r_{\min} = 2.0$. For $r_{\min} \geq 5.0$ the error bars on the fitting parameters become very large. The fitting results for $2.0 \geq r_{\min} \geq 4.0$ look stable, have small error bars, and are within the error bars of the points with larger $r_{\min}$. We therefore generally choose the fitting interval $r_{\min} = 3.0$ and $r_{\max} = 13.0$ for the result of μ and g^2.

B. Two flavors

For two degenerate light quark flavors on a $16^3 \times 4$ lattice there is a continuous crossover from the low-temperature chirally broken phase to the high-temperature plasma phase in which chiral symmetry is restored [4]. For a mass of $m = 0.025$ the center of the continuous transition curve is at $\beta = 5.291$.

For two quark flavors of mass $m = 0.025$ we have Wilson line correlation data of ordered start runs at β=5.293, 5.3, 5.4, and 5.6. Our evolutions show that for $\beta = 5.3$ the system is essentially in the chirally symmetric plasma phase. The correlation measurements at these four different values of β should give an indication of the temperature dependence of the heavy quark potential, and in particular of the screening mass, in the plasma phase.

Table I shows the parameters g^2 and μ of the potential (11) at $\beta = 5.293$ for several fitting ranges. This value of β is close to $\beta = 5.291$, where the largest fluctuations of $\langle \bar{\psi}\psi \rangle$ and the expectation value of the real part of the Wilson line $\langle \mathrm{Re}\, P \rangle$ have been observed [4,16]. The ordered start $\beta = 5.293$ run has 1000 units of time of which 800 have been included in the fitting process. The screening mass is relatively small which indicates that we are close to the transition region where long correlation lengths occur.

The $\beta = 5.3$ run has 1000 units of time, of which the first 200 have been discarded for equilibration. The evolution of $\langle \mathrm{Re}\, P \rangle$ for $\beta = 5.3$ still shows some remnants of the large fluctuations at $\beta = 5.291$. Figure 5 shows the heavy quark potential at $\beta = 5.3$ near the origin. The parameters of the fitted potential for several fitting ranges are listed in Table II.

The evolutions of $\langle \bar{\psi}\psi \rangle$ and $\langle \mathrm{Re}\, P \rangle$ for $\beta = 5.4$ are very stable. The heavy quark potential at $\beta = 5.4$ can be seen in Fig. 6, and Table III shows the fitting results for this value of β. The correlation data and the fitted function for a range $1.0 \leq r \leq 13.0$ is shown in Fig. 7. It is clear that the function does not match the data too well; especially the data points in the third and fifth bin are significantly higher than the fitting function. This situation is much improved if the fitting range starts from $r_{\min} = 2.0$ as is noticeable from Fig. 8. This behavior is typical for all fits.

The $\beta = 5.6$ potential is shown in Fig. 9. The data includes 900 units of time out of 1000. The resulting fitting parameters are listed in Table IV.

By looking at the potential close to the origin one can notice that points $\mathbf{r}$ which do not lie on one of the main axis of the lattice give a systematically different contribution to the potential than on-axis lattice points. An example of this is shown in Fig. 5 for the potential close to the origin at $\beta = 5.3$. Off-axis points such as the second and the third which correspond to $r = \sqrt{1+1}$ and $r = \sqrt{1+1+1}$ lie beneath the curve expected from on-axis points such as r=1.0, 2.0, and 3.0. This behavior is a manifestation of the significant breaking of rotational symmetry by the potential at short distances.

The effects of rotational symmetry violation on the screening mass can be studied quantitatively by directly calculating μ from the potential $V(r)$ for a series of lattice points $\mathbf{r}$. For two nearby lattice points the screening mass

TABLE I. Fits of the heavy quark potential in the plasma phase for $N_f = 2$, $m = 0.025$, $\beta = 5.293$, 800 units of time, ordered start.

Fitting range	g^2	μ	S
1.0–13.0	0.212 ± 0.015	0.609 ± 0.056	8.7
2.0–13.0	0.145 ± 0.023	0.457 ± 0.070	4.0
3.0–13.0	0.155 ± 0.048	0.468 ± 0.097	3.8
4.0–13.0	0.233 ± 0.153	0.530 ± 0.151	3.7

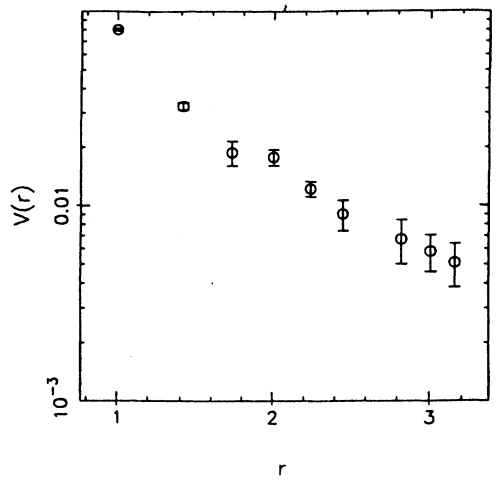

FIG. 5. Static interquark potential near the origin for $N_f = 2$, $m = 0.025$, $\beta = 5.3$.

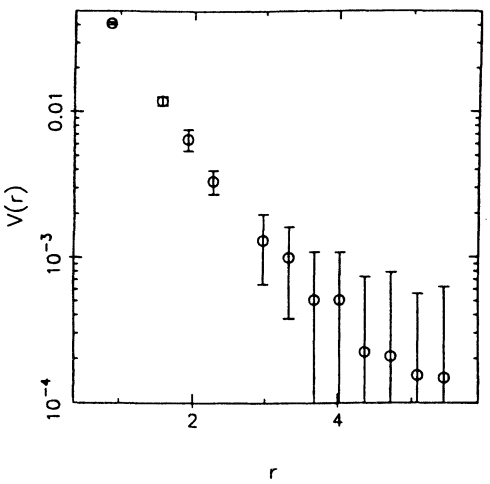

FIG. 6. Static interquark potential for $N_f = 2$, $m = 0.025$, $\beta = 5.4$.

TABLE II. Fits of the heavy quark potential in the plasma phase for $N_f = 2$, $m = 0.025$, $\beta = 5.3$, 800 units of time, ordered start.

Fitting range	g^2	μ	S
1.0–4.0	0.210 ± 0.012	0.934 ± 0.079	8.2
1.0–5.0	0.204 ± 0.013	0.907 ± 0.087	10.4
2.0–5.0	0.108 ± 0.018	0.589 ± 0.106	1.5
3.0–6.0	0.100 ± 0.015	0.554 ± 0.099	2.3
1.0–13.0	0.199 ± 0.015	0.887 ± 0.095	17.0
2.0–13.0	0.097 ± 0.018	0.541 ± 0.109	6.4
3.0–13.0	0.076 ± 0.013	0.482 ± 0.085	5.7
4.0–13.0	0.082 ± 0.003	0.495 ± 0.098	5.4

TABLE III. Fits of the heavy quark potential in the plasma phase for $N_f = 2$, $m = 0.025$, $\beta = 5.4$, 1800 units of time, ordered start.

Fitting range	g^2	μ	S
1.0–4.0	0.188 ± 0.002	1.471 ± 0.015	29.6
1.0–5.0	0.187 ± 0.002	1.467 ± 0.017	31.3
2.0–5.0	0.134 ± 0.015	1.183 ± 0.053	2.7
3.0–6.0	0.061 ± 0.030	0.904 ± 0.146	1.9
1.0–13.0	0.187 ± 0.002	1.466 ± 0.018	40.5
2.0–13.0	0.129 ± 0.017	1.165 ± 0.061	11.7
3.0–13.0	0.063 ± 0.035	0.913 ± 0.174	9.8
4.0–13.0	0.051 ± 0.099	0.857 ± 0.418	9.3

TABLE IV. Fits of the heavy quark potential in the plasma phase for $N_f = 2$, $m = 0.025$, $\beta = 5.6$, 900 units of time, ordered start.

Fitting range	g^2	μ	S
1.0–4.0	0.135 ± 0.005	1.632 ± 0.038	19.2
1.0–5.0	0.135 ± 0.005	1.629 ± 0.038	19.7
2.0–5.0	0.121 ± 0.031	1.419 ± 0.121	1.9
3.0–6.0	0.219 ± 0.203	1.559 ± 0.292	2.5
1.0–13.0	0.135 ± 0.005	1.630 ± 0.039	32.0
2.0–13.0	0.129 ± 0.034	1.449 ± 0.130	15.0
3.0–13.0	0.260 ± 0.212	1.612 ± 0.270	14.2
4.0–13.0	0.255 ± 0.253	2.696 ± 0.649	13.0

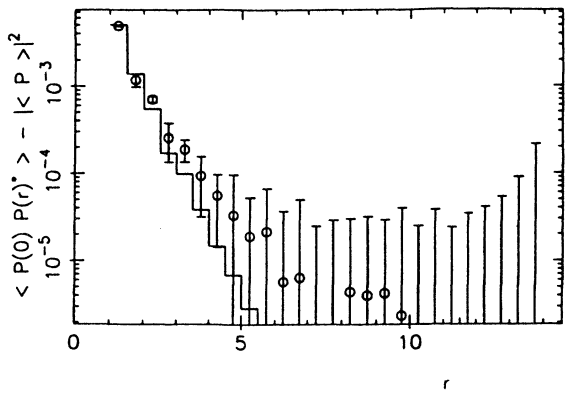

FIG. 7. Wilson line correlation fit for $N_f = 2$, $m = 0.025$, $\beta = 5.4$. The lower fitting range is $r_{\min} = 1.0$. The data shown are binned into intervals of $\Delta r = 0.5$.

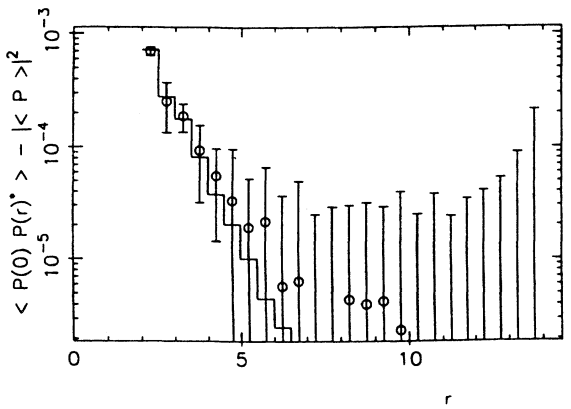

FIG. 8. Wilson line correlation fit for $N_f = 2$, $m = 0.025$, $\beta = 5.4$. The lower fitting range is $r_{\min} = 2.0$. The data shown are binned into intervals of $\Delta r = 0.5$.

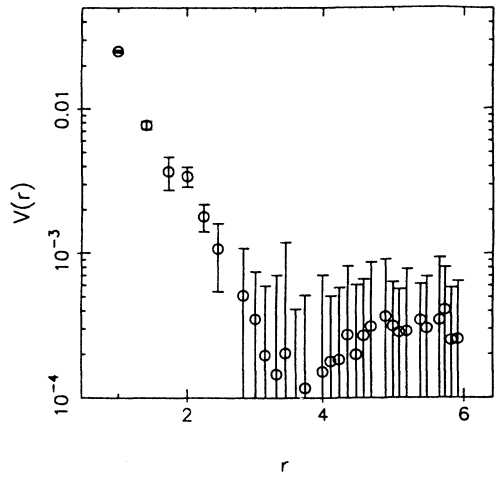

FIG. 9. Static interquark potential for $N_f = 2$, $m = 0.025$, $\beta = 5.6$.

can be obtained from ratios of the potential at distances r_1 and r_2:

$$\mu(r_1, r_2) = \frac{1}{r_2 - r_1} \ln \frac{r_1}{r_2} \frac{V(r_1)}{V(r_2)} . \tag{13}$$

Values for μ obtained from formula (13) are listed in Table V.

The screening masses obtained from on-axis points [$\mu(1,2)$, $\mu(2,3)$, and $\mu(3,4)$] agree quite well with the fitted values of Table II. It is clear, however, that for $1 \leq r \leq 2$ rotational symmetry is strongly broken. The value for μ in the lattice diagonal is 50% higher than the value on axis. For μ between 2 and 3 the discrepancy has somewhat diminished. The point $\sqrt{3^2+1}$ which is close to the axis agrees better with $\mu(2,3)$ than the points which are further out towards the diagonal. Going out to three lattice spacings it seems that rotational symmetry has been mainly restored; at this distance, however, the errors become very large.

In consistency with the fitting range dependence of the potential parameters we can conclude that in order to extract the asymptotic behavior of the potential we have to go out at least to three lattice spacing ($r_{\min} \geq 3.0$). Results for μ that include points near the origin should be regarded as giving some effective, short-distance screening mass.

A similar two-flavor calculation with a mass of $m = 0.025$ on a $12^3 \times 4$ lattice was carried out by Karsch and Wyld [12]. They measured Wilson line correlations for β=5.3, 5.4, 5.6, and 5.8.

There is very good agreement between the Karsch-Wyld and our data points for the heavy quark potential at β=5.3, 5.4, and 5.6 (our values are systematically a little lower, which can be explained by our bigger volume). There is, however, a rather large discrepancy between the values for the screening masses at $\beta = 5.4$ and 5.6. Karsch and Wyld obtain $\mu = 1.015 \pm 0.03$ at $\beta = 5.4$ and $\mu = 1.210 \pm 0.003$ at $\beta = 5.6$ by fitting from $r = 1.0$ to $r = 3.5$. This is to be compared with our values for μ in Tables III and IV.

After a detailed investigation it turned out that the discrepancy seems to come from a difference in the error bars between the two calculations. It seems that our relative errors for the first few points in Fig. 8 are smaller than those of Karsch and Wyld. By starting the fit with the parameter values of Karsch and Wyld one can watch the fitting routine minimize the function S by converging to our larger value for μ.

As pointed out above, rotational symmetry is broken near the origin. Because of their smaller lattice Karsch and Wyld have to include points near the origin in their fits which can significantly affect the results. Their values for μ can be considered as effective screening masses near the origin. We think that points close to the origin should be discarded for the fitting process and regard the values obtained for $r_{\min} \geq 3.0$ as the results for the screening mass μ.

C. Three flavors

For three quark flavors of mass $m = 0.025$ we have Wilson line correlation data at β=5.14, 5.24, and 5.44. The β values for $N_f = 3$ have been chosen to correspond to the $N_f = 2$ values such that they differ by the critical couplings. This way a comparison between two and three flavors can be made.

The potentials for $\beta = 5.14$ and 5.44 are shown in Figs. 10 and 11. For every value of β we have 2000 measurements taken at the end of each trajectory of $\frac{1}{2}$ unit of time; the first 200 measurements are part of the equilibration process and have not been included in our data. In Tables VI–VIII we list the fitting results for the $q\bar{q}$

TABLE V. Rotational dependence of the screening mass for $N_f = 2$, $m = 0.025$, $\beta = 5.3$.

$\mu(1,2)$	=	0.84 ± 0.10	$\mu(2,3)$	=	0.70 ± 0.22
$\mu(1,\sqrt{1+1})$	=	1.42 ± 0.05	$\mu(2,\sqrt{2^2+1+1})$	=	1.09 ± 0.20
$\mu(1,\sqrt{1+1+1})$	=	1.26 ± 0.15	$\mu(2,\sqrt{2^2+2^2})$	=	1.03 ± 0.27
$\mu(1,\sqrt{2^2+1})$	=	0.93 ± 0.11	$\mu(2,\sqrt{3^2+1})$	=	0.65 ± 0.27
$\mu(3,4)$			=		0.46 ± 0.51
$\mu(3,\sqrt{3^2+3^2})$			=		0.42 ± 0.61
$\mu(3,\sqrt{3^2+2^2+2^2})$			=		0.47 ± 0.49
$\mu(3,\sqrt{3^2+3^2+1})$			=		0.59 ± 0.76

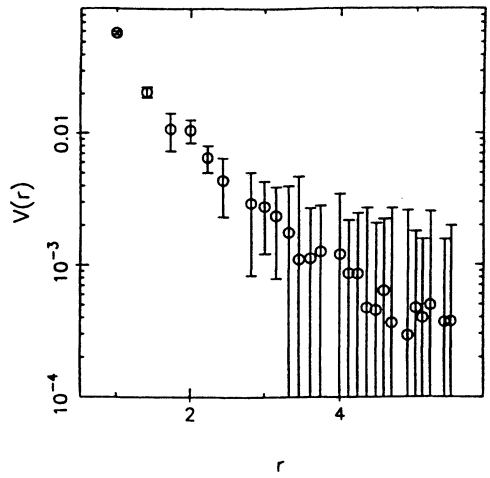

FIG. 10. Static interquark potential for $N_f = 3$, $m = 0.025$, $\beta = 5.14$.

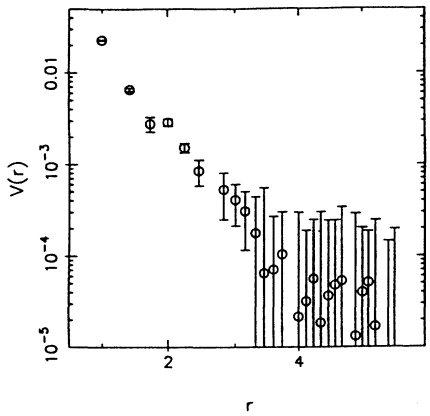

FIG. 11. Static interquark potential for $N_f = 3$, $m = 0.025$, $\beta = 5.44$.

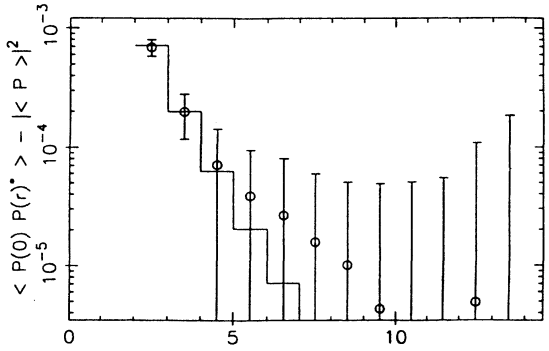

FIG. 12. Wilson line correlation fit for $N_f = 3$, $m = 0.025$, $\beta = 5.14$. The lower fitting range is $r_{\min} = 2.0$. The data shown are binned into intervals of $\Delta r = 1.0$.

TABLE VI. Fits of the heavy quark potential in the plasma phase for $N_f = 3$, $m = 0.025$, $\beta = 5.14$, 900 units of time, ordered start.

Fitting range	g^2	μ	S
1.0–13.0	0.211 ± 0.012	1.254 ± 0.078	14.5
2.0–13.0	0.103 ± 0.022	0.837 ± 0.136	6.2
3.0–13.0	0.042 ± 0.018	0.569 ± 0.123	5.4
4.0–13.0	0.025 ± 0.015	0.476 ± 0.129	4.9

TABLE VII. Fits of the heavy quark potential in the plasma phase for $N_f = 3$, $m = 0.025$, $\beta = 5.24$, 900 units of time, ordered start.

Fitting range	g^2	μ	S
1.0–13.0	0.200 ± 0.007	1.713 ± 0.038	115.7
2.0–13.0	0.146 ± 0.060	1.403 ± 0.187	60.8
3.0–13.0	0.190 ± 0.407	1.423 ± 0.615	56.3
4.0–13.0	0.323 ± 2.529	1.514 ± 0.748	54.6

TABLE VIII. Fits of the heavy quark potential in the plasma phase for $N_f = 3$, $m = 0.025$, $\beta = 5.44$, 900 units of time, ordered start.

Fitting range	g^2	μ	S
1.0–13.0	0.145 ± 0.004	1.813 ± 0.029	87.2
2.0–13.0	0.239 ± 0.049	1.864 ± 0.106	45.6
3.0–13.0	0.476 ± 1.778	1.988 ± 0.557	43.8
4.0–13.0	0.00033 ± 1.48	1.477 ± 0.194	42.6

TABLE IX. Fits of the heavy quark potential in the plasma phase for $N_f = 4$, $m = 0.025$, $\beta = 4.99$, 3000 units of time, ordered start.

Fitting range	g^2	μ	S
1.0–13.0	0.213 ± 0.008	1.537 ± 0.043	20.3
2.0–13.0	0.069 ± 0.019	0.880 ± 0.133	5.3
3.0–13.0	0.017 ± 0.004	0.477 ± 0.084	3.5
4.0–13.0	0.011 ± 0.003	0.408 ± 0.066	3.3
5.0–13.0	0.009 ± 0.007	0.376 ± 0.098	3.1

TABLE X. Fits of the heavy quark potential in the plasma phase for $N_f = 4$, $m = 0.0375$, $\beta = 5.02$, 2200 units of time, ordered start.

Fitting range	g^2	μ	S
1.0–13.0	0.188 ± 0.006	1.334 ± 0.044	16.7
2.0–13.0	0.064 ± 0.008	0.742 ± 0.055	4.1
3.0–13.0	0.035 ± 0.008	0.568 ± 0.066	3.1
4.0–13.0	0.032 ± 0.019	0.547 ± 0.122	2.9
5.0–13.0	0.028 ± 0.101	0.527 ± 0.316	2.8

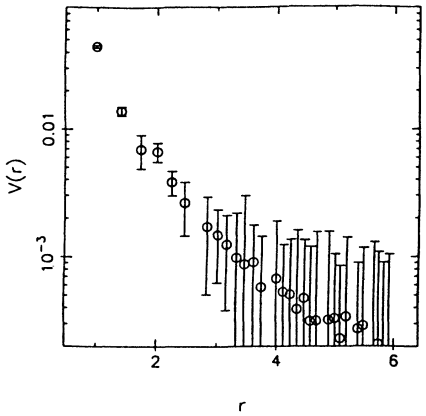

FIG. 13. Static interquark potential for $N_f = 4$, $m = 0.025$, $\beta = 4.99$.

potential of the form (11) for the three values of β. A fitting example is shown in Fig. 12.

D. Four flavors

For four quark flavors on a $16^3 \times 4$ lattice a first-order transition is seen for mass values of $m = 0.01$, 0.025, 0.0375, and 0.05 [5,17].

We have measured Wilson line correlations in the plasma phase for $m = 0.025$, 0.0375, and 0.05 right at or very close to the transition.

For $m = 0.025$ the transition is at $\beta = 4.99$. At this value we have measurements from 3000 units of time starting from an ordered configuration.

For $m = 0.0375$ the transition is at $\beta = 5.02$. Here we have 2500 units of time from which the first 300 have been discarded for the fits.

For a mass value of $m = 0.05$ we first ran each 1000 units of time with an ordered and disordered start at $\beta = 5.04$ and the evolutions stayed apart. As we extended the ordered start run, however, it tunneled to the disordered phase after 1500 units of time. In order to avoid tunneling we raised β by 0.005 and ran a ordered start run at $\beta = 5.045$ for 2500 units of time. We have included 2250 units of time in our fits. The values of μ for the 1000 units of time at $\beta = 5.04$ and the 2500 units of time agree within errors (the values for $\beta = 5.04$ are $\sim 25\%$ lower than those for $\beta = 5.045$).

Tables IX–XI summarize the fitting results for the three different masses.

Figures 13 and 14 show the $q\bar{q}$ potential for $m = 0.025$ and 0.05 in the plasma phase right at or very close to the transition. For $m = 0.025$ the Wilson line correlation data and the fitted function for a range $2.0 \leq r \leq 13.0$ is shown in Fig. 15.

TABLE XI. Fits of the heavy quark potential in the plasma phase for $N_f = 4$, $m = 0.05$, $\beta = 5.045$, 2250 units of time, ordered start.

Fitting range	g^2	μ	S
1.0–13.0	0.144 ± 0.015	0.889 ± 0.125	12.2
2.0–13.0	0.054 ± 0.017	0.447 ± 0.162	2.2
3.0–13.0	0.044 ± 0.019	0.405 ± 0.167	1.8
4.0–13.0	0.045 ± 0.033	0.407 ± 0.205	1.7
5.0–13.0	0.054 ± 0.063	0.429 ± 0.238	1.6

V. COMPARISONS

In this section we summarize and compare our main results for the interquark potential in the plasma phase.

For two and three flavors we have listed in Table XII and XIII the temperature dependence of the screening mass μ near the transition region. For four flavors the values of μ for different quark masses at the transition are shown in Table XIV. For the two- and four-flavor tables we have selected the fitting range [3.0–13.0]. For three flavors the fitting range is [2.0–13.0]. For these ranges the fitting results are stable and have the smallest error bars.

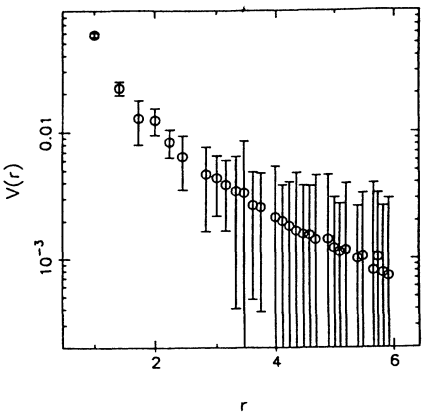

FIG. 14. Static interquark potential for $N_f = 4$, $m = 0.05$, $\beta = 5.045$.

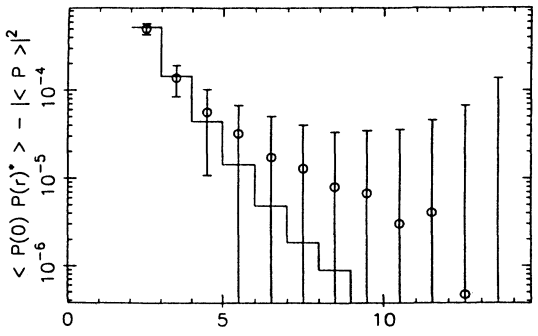

FIG. 15. Wilson line correlation fit for $N_f = 4$, $m = 0.025$, $\beta = 4.99$. The lower fitting range is $r_{\min} = 2.0$. The data shown are binned into intervals of $\Delta r = 1.0$.

TABLE XII. Temperature dependence of screening masses for $N_f = 2$, $m = 0.025$. Fitting range 3.0–13.0.

β	μ
5.3	0.482 ± 0.085
5.4	0.913 ± 0.174
5.6	1.612 ± 0.270

For both two and three flavors we recognize a strong temperature dependence of μ. This dependence seems to be stronger than previous results suggest [15,12]. Taking scaling violations into account, the β values for $N_f = 2$ correspond according to [12] to $T/T_c \simeq 1.1$, 1.4, and 2.0. If we define $m_D = \mu/a$ then the perturbative form in Eq. (9) predicts that $m_D/T \simeq$ const. Since $m_D/T = 4\mu$ it follows that μ should be constant. This, however, is clearly not the case for our values of the lattice screening masses so that the perturbation theory results and our lattice calculations do not seem to be compatible in the temperature regime close to the transition.

According to [11], perturbation theory predicts that for $T/T_c = 1$, $\mu = 0.42$, and that $c\bar{c}$ becomes unbound for $T \simeq 2T_c$ which corresponds to $\mu = 0.75$. Our results for $N_f = 3$ and $\beta = 5.14$ give $\mu = 0.837 \pm 0.136$, suggesting that J/ψ suppression might be effective for temperatures $T \simeq T_c$.

Screening masses for pure QCD have been measured on a $24^3 \times 4$ lattice with the Columbia 64-node machine. These are some of the results: $\mu = 0.162 \pm 0.017$ for $\beta_c = 5.6925$, $\mu = 0.313 \pm 0.033$ for $\beta = 5.70$, and $\mu = 0.635 \pm 0.039$ for $\beta = 5.75$.

If we compare the screening masses at $\beta = 5.70$ for pure QCD and at $\beta = 5.3$ for $N_f = 2$ QCD (in both cases $\beta - \beta_c \simeq 0.008$) we see that the value for μ is $\sim 50\%$ larger in the full theory than in pure gauge theory. This is quite comparable to the 30% found by [15]. For larger values of β ($T \simeq 2T_c$) we find for $N_f = 2$ that $\mu/T \simeq 6.5$ whereas for pure SU(3) gauge theory $\mu/T \simeq 3$ [18].

This shows that the inclusion of light dynamical fermions enhances the screening effects significantly.

This behavior is confirmed by comparing the screening masses between $N_f = 2$ and $N_f = 3$. As expected we see an increase of μ when changing from two to three flavors at comparable values of β [$\beta(N_f = 2) \simeq \beta(N_f = 3) + 0.16$]. The addition of a fermion flavor causes stronger color screening of the heavy quarks.

As Table XIV shows there is no clear variation of μ for four flavors as the quark mass is lowered from $m = 0.05$ to $m = 0.025$.

TABLE XIII. Temperature dependence of screening masses for $N_f = 3$, $m = 0.025$. Fitting range 2.0–13.0.

β	μ
5.14	0.837 ± 0.136
5.24	1.403 ± 0.187
5.44	1.864 ± 0.106

TABLE XIV. Quark mass dependence of screening masses for $N_f = 4$ at the transition. Fitting range 3.0–13.0.

m	β	μ
0.025	4.99	0.477 ± 0.084
0.0375	5.02	0.568 ± 0.066
0.05	5.045	0.405 ± 0.167

In fact, the results are consistent with μ being constant. This suggests that we have reached the chiral limit in our lattice calculation; that is, our value of $\mu = 0.477 \pm 0.084$ is within errors very likely equal to the $m = 0$ value of μ.

VI. CONCLUSIONS

High statistics measurements of Wilson line correlation functions have us allowed to obtain some detailed information about the heavy quark potential.

We have studied interquark forces in both the confined and plasma phase of QCD on a $16^3 \times 4$ lattice. In the low-temperature phase the important effects of dynamical quark loops manifest themselves in the cutoff of the linearly rising interquark potential for a lattice distance $r \geq 4$. In the chirally symmetric high-temperature phase we have performed a systematic study of the temperature, flavor, and mass dependence of the screening mass μ.

The screening mass is one of the quantities accessible by lattice QCD which is most likely to directly affect heavy ion experiments. Our analysis yields $\mu = 0.837 \pm 0.136$ for three quark flavors at $T \simeq T_c$ which suggests that J/ψ suppression might be effective for temperatures slightly above the transition.

We also were able to demonstrate that color screening enhances the value of μ by 50% for $N_f = 2$ full QCD over that in pure gauge theory. This effect increases if additional quark flavors are added.

Our results about the heavy quark potential are consistent with earlier work and extend it in several ways. We have a larger lattice, smaller quark masses, and more statistics than in previous calculations. The larger lattice and increased statistics have allowed us to include larger distances in our fits and thereby better incorporate the asymptotic behavior of the interquark potential. In addition, we were able to investigate the restoration of rotational symmetry on the lattice.

ACKNOWLEDGMENTS

The author would like to thank Professor N. Christ for the supervision of this work and F. Brown, F. Butler, H. Chen, Z. Dong, M. Gao, P. Hsieh, W. Schaffer, and A. Vaccarino for their collaboration. Financial support by the Swiss Academy of Sciences and the U.S. Department of Energy is gratefully acknowledged.

[1] T. Matsui and H. Satz, Phys. Lett. B **178**, 416 (1986).
[2] J. B. Kogut, Rev. Mod. Phys. **55**, 775 (1983).
[3] G. Parisi, R. Petronzio, and F. Rapuano, Phys. Lett. B **128**, 418 (1983).
[4] F. R. Brown *et al.*, Phys. Rev. Lett. **65**, 2491 (1990).
[5] F. R. Brown *et al.*, Phys. Lett. B **251**, 181 (1990).
[6] F. Butler, in *Lattice '88*, Proceedings of the International Symposium, Batavia, Illinois, 1988, edited by A. S. Kronfeld and P. B. Mackenzie [Nucl. Phys. B (Proc. Suppl.) **9**, 557 (1989)]; N. H. Christ, in *Lattice '89*, Proceedings of the International Symposium, Capri, Italy, 1989, edited by R. Petronzio *et al.* [Nucl. Phys. B (Proc. Suppl.) **17**, 267 (1990)]; A. Vaccarino, *ibid.*, p. 421.
[7] M. Fukugita, in *Lattice Gauge Theory Using Parallel Processors*, Proceedings of the CCAST Symposium, Beijing, China, 1987, edited by X. Y. Li, Z. M. Qiu, and H. C. Ren (Gordon and Breach, New York, 1987), p. 195.
[8] R. Gupta, in *Lattice Gauge Theory Using Parallel Processors* [7], p. 449.
[9] M. Gao, Ph.D. thesis, Columbia University, 1989.
[10] M. Faber, P. De Forcrand, H. Markum, M. Meinhart, and I. Stamatescu, Phys. Lett. B **200**, 348 (1988).
[11] F. Karsch, M. T. Mehr, and H. Satz, Z. Phys. C **37**, 617 (1988).
[12] F. Karsch and H. W. Wyld, Phys. Lett. B **213**, 505 (1988).
[13] S. Nadkarni, Phys. Rev. D **27**, 917 (1983); **33**, 3738 (1986).
[14] N. Attig, F. Karsch, B. Petersson, H. Satz, and U. Wolff, Phys. Lett. B **209**, 65 (1988).
[15] R. V. Gavai, M. Lev, B. Petersson, and H. Satz, Phys. Lett. B **203**, 295 (1988).
[16] L. I. Unger, Ph.D. thesis, Columbia University, 1990.
[17] A. Ukawa, in *Non-Perturbative Aspects of the Standard Model*, Proceedings of the Workshop, Jaca, Spain, 1988, edited by J. Abad *et al.* [Nucl. Phys. B (Proc. Suppl.) **10A**, 66 (1989)]; S. Gottlieb *et al.*, Phys. Rev. D **35**, 2531 (1987); **35**, 3972 (1987); in *Field Theory on the Lattice*, Proceedings of the International Symposium, Seillac, France, 1987, edited by A. Billoire *et al.* [Nucl. Phys. B (Proc. Suppl.) **4**, 294 (1988)].
[18] T. A. DeGrand and C. E. DeTar, Phys. Rev. D **34**, 2469 (1986); N. Attig *et al.*, Phys. Lett. B **209**, 65 (1988).